Head and Neck Pathol (2011) 5:205–215
DOI 10.1007/s12105-011-0260-4

ORIGINAL PAPER

# Orbital Infantile Myofibroma: a Case Report and Clinicopathologic Review of 24 Cases from the Literature

**Corey J. Mynatt · Kenneth A. Feldman · Lester D. R. Thompson**

Received: 23 February 2011 / Accepted: 1 April 2011 / Published online: 22 April 2011


**Abstract** Isolated orbital infantile myofibroma are rare tumors in the head and neck. The mass-like clinical presentation and variable histologic features result in frequent misdiagnosis and potentially inappropriate clinical management. There are only a few reported cases in the English literature. Twenty-four patients with orbital infantile myofibroma or myofibromatosis were compiled from the English literature (Medline 1960–2011) and integrated with this case report. The patients included 14 males and 10 females, aged newborn to 10 years (mean, 34.8 months), who presented with a painless mass in the infra- or supra-orbital regions, usually increasing in size andassociated with exophthalmos ($n = 5$). Females were on average older than their male counterparts (38.9 vs. 31.9 months, respectively; $P = 0.71$). The tumors were twice as frequent on the left ($n = 16$) than right ($n = 8$). Patients experienced symptoms for an average of 2.7 months before clinical presentation. The tumors involved the bone ($n = 17$) or the soft tissues ($n = 7$) of the orbit, with extension into the nasal or oral cavity ($n = 3$). The mean size was 3.0 cm, with a statistically significant difference between males and females (mean: 3.9 vs. 1.82; $P = 0.0047$), but without any differences based on age at presentation ($P = 0.25$), duration of symptoms ($P = 0.66$), or bone or soft tissue involvement ($P = 0.51$). Grossly, all tumors were well-circumscribed, firm to rubbery, homogenous, and white–grey. Histologically, the tumors were biphasic, showing whorled and nodular areas of fusiform cells with extracellular collagen, mixed with a population of small, primitive-appearing, darkly staining cells. Necrosis was not present, but mitoses could be seen. Tumors with immunohistochemistry performed showed strong and diffuse smooth muscle actin and vimentin immunoreactivity, but were negative with muscle specific actin, desmin, MYOD1, myogenin, S100 protein, GFAP, keratin, CD31, 34, Factor VIIIR-Ag, and CD45RB. The principle histologic differential diagnosis includes juvenile hyaline fibromatosis, fibrous hamartoma of infancy, fibromatosis coli, leiomyoma, infantile hemangiopericytoma, infantile fibrosarcoma, Ewing sarcoma/primitive neuroectodermal tumor, and lymphoma. All patients were managed with surgery. Recurrences developed in two patients at 4 and 6 months, respectively. Follow-up data was available on all but two patients ($n = 22$). These patients were either alive without evidence of disease ($n = 18$), alive but with disease ($n = 3$), or had died unrelated to this disease (i.e., neuroblastoma, $n = 1$). Orbital infantile myofibroma is a rare tumor, presenting in infancy as an enlarging mass of the orbit, with characteristic histomorphologic and immunophenotypic features. Orbital disease is usually isolated rather than part of systemic disease, and shows an excellent long-term prognosis, making appropriate separation from other conditions important.

**Keywords** Infantile myofibroma · Myofibromatosis · Juvenile fibromatosis · Orbit · Soft tissue · Infancy · Pediatrics · Immunohistochemistry · Prognosis · Survival · Differential diagnosis · Fibromatosis

C. J. Mynatt · L. D. R. Thompson
Department of Pathology, Southern California Permanente Medical Group, Woodland Hills, CA, USA

K. A. Feldman
Department of Ophthalmology, Southern California Permanente Medical Group, Harbor City, CA, USA

L. D. R. Thompson (✉)
Department of Pathology, Woodland Hills Medical Center, Southern California Kaiser Permanente Group, 5601 De Soto Avenue, Woodland Hills, CA 91365, USA
e-mail: Lester.D.Thompson@kp.org

## Introduction

Soft tissue lesions of the head and neck, and specifically of the orbit, are quite uncommon. Moreover, soft tissue lesions in pediatric patients are rare and encompass distinct histologic entities. One of these tumors is infantile myofibroma or myofibromatosis. Infantile myofibroma is a nonencapsulated, nonmetastasizing, locally infiltrative lesion, considered to be part of the fibrous proliferations of infancy. This lesion has been referred to by numerous other names, including congenital generalized fibromatosis, congenital multiple fibromatosis, multiple mesenchymal hamartomas, diffuse congenital fibromatosis, and multiple vascular leiomyomas of the newborn, among others [1, 2]. Specifically, infantile myofibroma is a single lesion, while infantile myofibromatosis is used for multiple lesions or multifocal disease. While fibromatoses [3] may occur in any region of the body, many occur in the head and neck, usually involving the superficial soft tissues. Within the head and neck, infantile myofibromatosis, although a very rare lesion, seems to show a tendency to develop around the orbit [1–7] in the few cases reported in the English literature [4–18]. The rarity of this tumor poses a diagnostic challenge that may lead to a misdiagnosis and subsequent inappropriate patient management. This case report and literature review focuses on the clinical presentation, histologic features, immunohistochemical profile, and therapeutic management of orbital infantile myofibroma/myofibromatosis in relation to patient prognosis and outcome, with a comparison to the differential diagnosis for this entity.

## Case Presentation

A 3-year-old boy presented to his pediatrician with a 3-month history of a mass at the temporal aspect of the left orbital rim, immediately beneath the lateral aspect of the eyebrow. The parents and the patient did not recall any history of trauma. The mass was felt to be slowly increasing in size. The patient's past medical history was significant only for slightly delayed speech development. On physical examination, the approximately 2 cm mass was noted to be firm and immobile, without overlying erythema. The rest of the exam was unremarkable. A referral to pediatric ophthalmology showed an entirely normal eye exam. Although a traumatic subperiosteal hematoma was suspected, further work-up was pursued due to the duration of the mass, the lack of trauma history, and the increase in size. A computed tomography (CT) scan of the orbits revealed an expansile, osteolytic, soft tissue mass measuring approximately 1.5 cm in the superolateral margin of the left bony orbit (Fig. 1). The mass was relatively well-marginated but demonstrated bony destruction of the superolateral orbital wall and the outer lateral margin of the involved zygomatic process of the frontal bone. In addition, the mass appeared to encroach onto the lacrimal gland. Magnetic resonance imaging (MRI) of the orbits revealed a well-marginated, ovoid, expansile, osteolytic mass in the superolateral left bony orbit measuring approximately 1.5 cm. The mass was isointense to brain parenchyma on T1-weighted images and hyperintense to brain parenchyma on T2-weighted images. After administration of gadolinium contrast, the mass demonstrated marked homogeneous enhancement (Fig. 2). There was loss of the adjacent cortical margins at the medial and lateral aspects of the mass. The clinical presentation combined with radiographic findings of an erosive, lytic lesion was thought to be most suggestive of Langerhans cell histiocytosis; however, the differential also included a fibro-osseous lesion (including fibrous dysplasia, juvenile ossifying fibroma, infantile fibrosarcoma), and metastatic disease (neuroblastoma, Wilms tumor, Ewing/PNET).

A referral was made for oculoplastic evaluation and orbitotomy with biopsy of the lesion. The patient was taken to the operating room for biopsy. An incision was made at the superior aspect of the lateral brow cilia overlying the bony mass. The adjacent periosteum was elevated, and no break in bone was encountered on the anterior surface of the skull. Dissection into the orbit revealed a lytic lesion

**Fig. 1** A CT scan of the orbit showing an expansile osteolytic soft tissue lesion at the superolateral margin of the *left* orbit, with bony destruction of the superolateral orbit wall

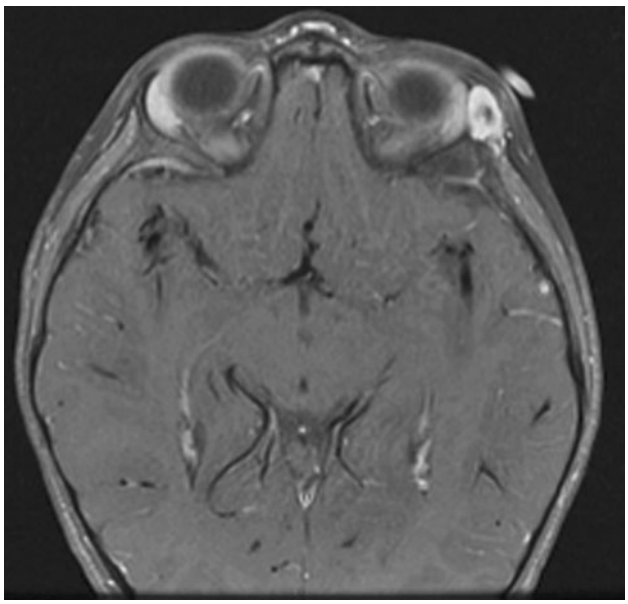

**Fig. 2** This T2 weighted MRI demonstrates a hyperintense mass immediately adjacent to the *left* globe, demonstrating focal central degeneration

just inside the orbital rim. A curette was used to evacuate the contents of the lytic space and this specimen was submitted to pathology. The biopsy material consisted of five fragments of tissue, ranging from 0.2 cm to 0.6 cm in greatest dimension, rubbery to firm and seemingly well-defined (circumscribed). There was a slightly degenerated, reddish appearance to the center of the tissue fragments. A portion of this tissue was submitted for frozen section examination to assess for adequacy. By microscopic examination, there was a biphasic appearance to the lesion (Fig. 3). There was a multinodular growth of numerous plump, myoid-type spindled cells with abundant eosinophilic cytoplasm arranged in short fascicles (Fig. 4). The nuclei were elongated and tapering (Fig. 5) with no significant nuclear atypia. There was a suggested hemangiopericytoma-like pattern (Fig. 6). The spindled cells were associated with areas of more myxoid background stroma, along with some areas that were more hyalinized. In addition, juxtaposed to the spindled cell population, was a primitive, "small round blue cell" population (Fig. 7). These cells were small, round with a very high nuclear-to-cytoplasmic ratio, eosinophilic cytoplasm, and indistinct cell borders (Fig. 8), arranged in a sheet-like to pseudorosette pattern. Focal areas showed tumor cell spindling. Glial-like tissue was suggested between the cells (Figs. 7, 8) and a suggestion of cilia was also noted in a few areas. Mitoses and necrosis were notably absent. Both of the morphologic patterns were immediately juxtaposed to bony fragments, the latter showing changes of remodeling (consistent with the radiographic findings).

The lesional cells showed strong immunoreactivity with vimentin and smooth muscle actin (Fig. 9), but were non-reactive with muscle markers (muscle specific actin, desmin, MYOD1, myogenin), S-100 protein, GFAP, NFP, keratin, CD99, and vascular markers (CD31, 34, Factor

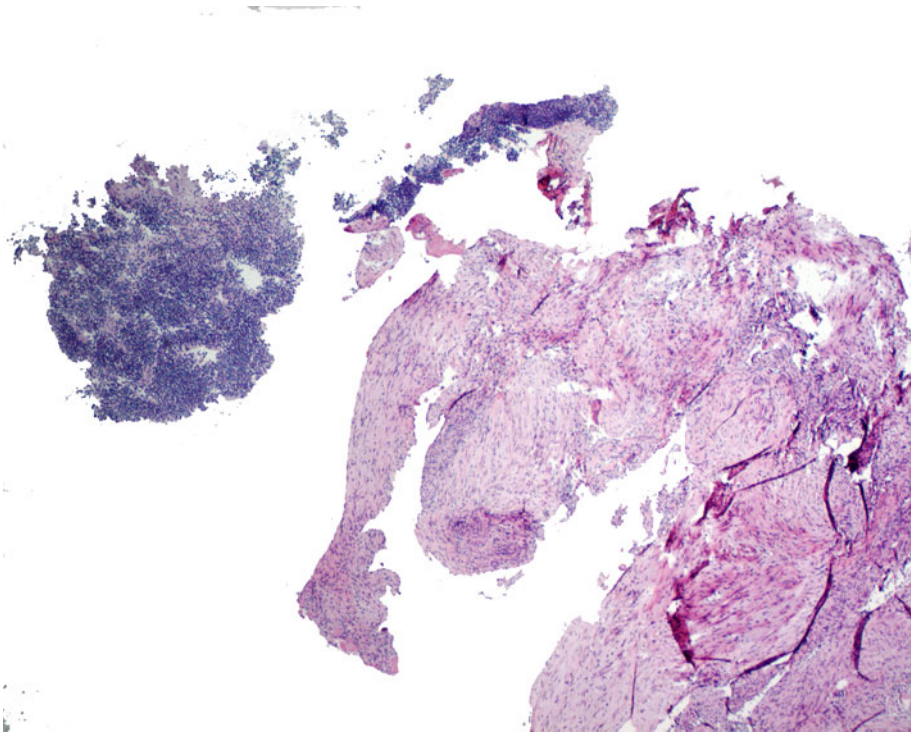

**Fig. 3** The biphasic appearance of the tumor is highlighted in this photomicrograph. The "small round blue cell" compartment on the *left*, while the more fibrous connective tissue compartment is on the *right*

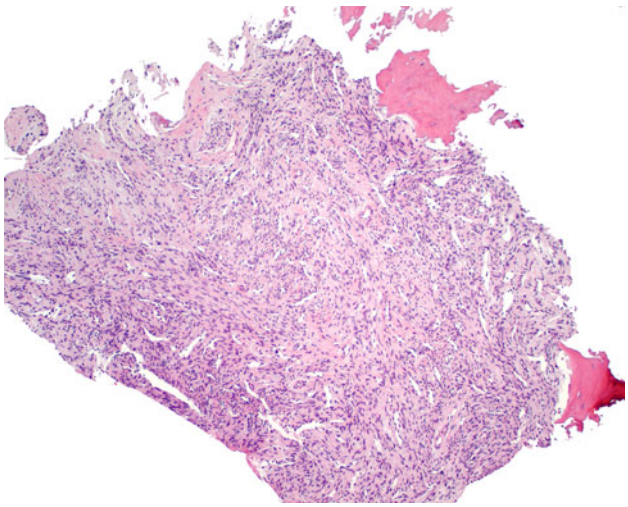

**Fig. 4** A myoid-type spindled cell population is noted, arranged in a vague fascicular architecture, with a rich vascular plexus, creating a "hemangiopericytoma-like" appearance. Note the fragments of bone at the periphery

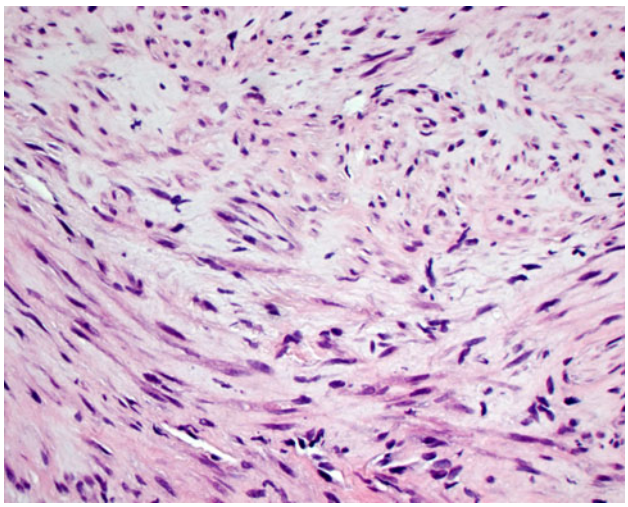

**Fig. 5** The elongated spindled cells with abundant, eosinophilic cytoplasm, creating a "myoid" appearance to the cells

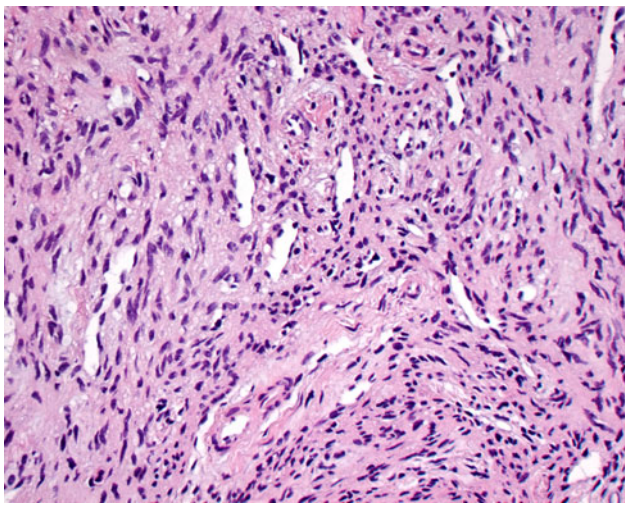

**Fig. 6** Open vascular channels could be seen within the spindled cell proliferation. Note the lack of cytologic atypia

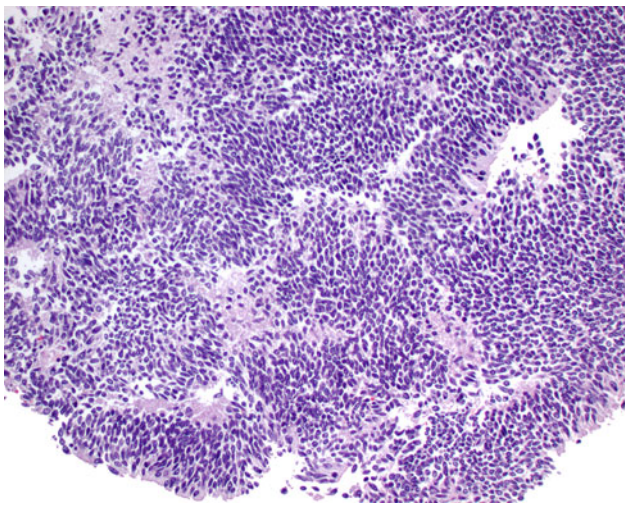

**Fig. 7** The primitive, almost blastema-like appearance to the second population of cells. Note the pseudorosette-like structures and the suggestion of "neural" matrix

VIIIR-Ag). Ki-67 showed no significant staining. Immunophenotypic analysis was performed by a standardized Envision™ method employing 4 μm-thick, formalin-fixed, paraffin-embedded sections. Table 1 documents the pertinent, commercially available immunohistochemical antibody panel used. When required, proteolytic antigen retrieval was performed by predigestion for 3 min with 0.05% Protease VIII (Sigma Chemical Co., St. Louis, MO) in a 0.1 M phosphate buffer, pH of 7.8, at 37°C. Heat induced epitope retrieval was performed, as required, by using formalin-fixed, paraffin-embedded tissue treated with a buffered citric acid solution at pH 6.0 (Citra, Dako Corporation, Carpinteria, CA) and heated for 20 min in a steamer. Standard positive controls were used throughout, with serum used as the negative control. The antibody reactions were described as either positive or negative. Glycogen was not identified (PAS with diastase).

Based on this aggregate of findings, a diagnosis of infantile myofibroma was made. After diagnosis, our patient was referred to a pediatric oncologist for evaluation. A bone scan and a CT scan of the chest, abdomen and pelvis failed to reveal evidence of multifocal disease. The decision of the family and managing physicians was made to observe the patient without further intervention, utilizing interval MRIs of the orbit every 3 months. Subsequent

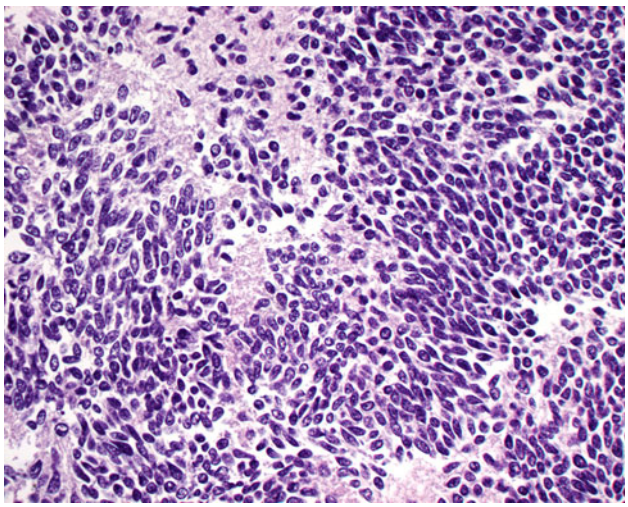

**Fig. 8** The cells have a very high nuclear to cytoplasmic ratio, focally with a matrix material in the background. However, the nuclei are bland without nucleoli and lacking mitoses

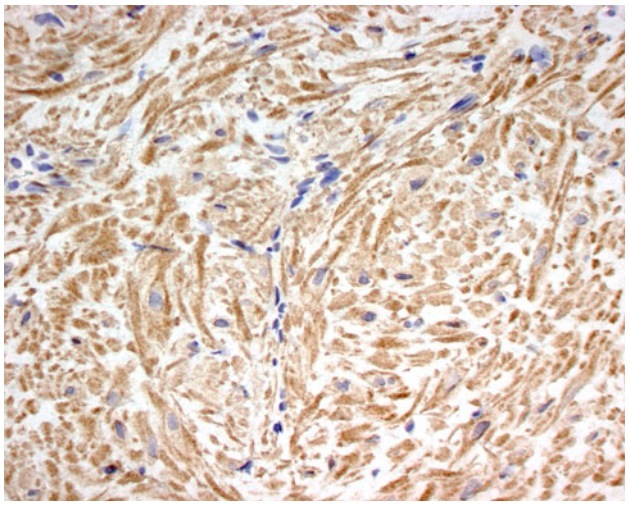

**Fig. 9** The lesional spindled cells show strong and diffuse smooth muscle actin immunoreactivity

MRIs with contrast of the orbits have shown progressive reduction in the size of the orbital rim lesion, without development of disease in any other location. At last follow-up, 12 months after initial diagnosis, the patient was doing well and managed by observation alone.

## Materials and Methods

A review of the English literature based on a MEDLINE search from 1966 to 2010 was performed and all cases of infantile myofibroma involving the orbit specifically were included in the review, the majority of which were single case reports [4–18]. Clinical series of "head and neck infantile myofibromatosis" were selected if critical information about orbit lesions was included. No foreign language articles were included, nor articles with limited or incomplete information [19, 20].

Categorical variables were analyzed using $\chi^2$ tests to compare observed and expected frequency distributions. Comparison of the mean between groups was made with independent $t$ tests (including 1-tailed and 2-tailed tests with degrees of freedom) or one-way analysis of variance, depending on whether there were two groups or more than two groups, respectively. Multiple comparisons were analyzed using the Tukey method. Confidence intervals of 95% were generated for all positive findings. The alpha level was set at $P < 0.05$.

## Definition and Nomenclature

Abnormal, nodular proliferations of fibrous connective tissue involving the dermis, muscle, bone, and viscera, presenting in newborns to young patients, was originally described by Stout et. al. as *generalized fibromatosis*, a subset of *juvenile fibromatosis* [3]. A few years earlier, a similar lesion was erroneously described as a congenital fibrosarcoma, even though identical to myofibroma, but quickly reclassified as a benign entity [21]. With more extensive evaluation and clinicopathologic correlation, infantile myofibromatosis was the new name given by Chung and Enzinger [1]. A number of specific features of the disorder were described:

(1) Development of the disease in infancy (<2 years) in the majority of patients (89%), with many present at birth (54%);
(2) The majority of cases presenting as solitary (74%) versus multicentric (26%) disease;
(3) The solitary form was more common in males and involved the skin and soft tissues of the head, neck, and trunk;
(4) The multicentric form seemed to affect females more frequently, but developed in bone, viscera, and soft tissues;
(5) The tumor cells were intermediate between fibroblasts and smooth-muscle cells, presenting a biphasic appearance in different parts of the same tumor;
(6) The vast majority of patients were alive without evidence of disease, although patients with visceral involvement were more likely to die from disease [1, 2, 12].

Needless to say, many of these parameters are still valid and important in the management and diagnosis of the disorder today. However, there are some differences when isolated disease in the orbit is evaluated, as shown in the discussion below.

**Table 1** Immunohistochemical panel

| Antigen/antibody | Type | Company | Dilution | Antigen recovery |
|---|---|---|---|---|
| Vimentin | mm | Santa Cruz Biotechnology, Santa Cruz, CA | 1:100 | n/a |
| Smooth muscle actin | mm | Sigma Chemical, St. Louis, MO | 1:400 | n/a |
| Muscle specific actin | mm | Ventana, Tucson, AZ | Neat | Protease digestion |
| Desmin | mm | Santa Cruz Biotechnology | 1:200 | Protease digestion |
| MYOD1 | mm | LifeSpan Biosciences, Seattle, WA | 1:400 | Protease digestion |
| Myogenin | mm | LifeSpan Biosciences | 1:200 | Protease digestion |
| S-100 protein | rp | Dako, Carpinteria, CA | 1:800 | n/a |
| GFAP | rp | Dako | 1:500 | n/a |
| Cytokeratin | | | | |
| AE1/AE3 | mm | Boehringer Mannheim Biochemicals, Indianapolis, IN | 1:50 | Protease digestion |
| LP34 | mm | Dako | 1:200 | Protease digestion |
| CD99 | mm | Abnova, Walnut, CA | Neat | n/a |
| CD31 | mm | Dako | 1:100 | Steam |
| CD34 | mm | BioGenex Labs, San Ramon CA | 1:40 | Steam |
| Factor VIII-RAg | rp | Dako | 1:50 | n/a |
| NFP | mm | Dako | 1:50 | Protease digestion |
| Ki-67 | mm | Immunotech, Westbrook, ME | 1:20 | Steam |

*mm* Mouse monoclonal; *rp* rabbit polyclonal

## Epidemiology and Clinical Presentation

Evaluation of orbital infantile myofibroma shows that while males were affected more frequently than females in this review (Table 2), there was not a statistically significant difference ($P = 0.8$). Patients ranged in age from newborn to 10 years. The median age was 12 months, with a mode in newborn patients, even though the mean was 34.8 months (Fig. 10). The mean was skewed by 5 patients who were 96–120 months at presentation. Our patient, presenting at 3 years of age, was on the older end of this spectrum. Females were on average older than their male counterparts (38.9 vs. 31.9 months, respectively), although this was not a statistically significant difference ($P = 0.71$). Patients presented with a mass lesion around the region of the orbit or eye. The masses could be wart-like, pedunculated, or ulcerated. The tumors were described as firm, painless, well-circumscribed to smooth, and round. Occasional tumors were said to have an indistinct boundary. In a number of cases, patients presented with ptosis, eye displacement, and proptosis. Patients also experienced strabismus, photophobia, headaches, nausea, and vomiting. Interestingly, the tumors were twice as frequent on the left ($n = 16$) than the right ($n = 8$), and there is no satisfactory explanation for this finding. At present, there is no known embryologic or developmental reason why there would be a difference in the side of tumor development. There were more tumors affecting the lower or inferior orbit ($n = 16$) than the upper or superior orbit (eyelid and eyebrow included; $n = 6$), which was a statistically significant finding ($P = 0.03$). As seen in our patient, all tumors involving the superior orbit affected only the left side ($n = 6$), although not statistically significant ($P = 0.10$). The tumors predominantly involved the bone ($n = 13$), or the orbital soft tissues ($n = 7$), and some showed an extension into adjacent structures, including the hard palate, paranasal sinuses, and parietal skull ($n = 4$). There were no statistically significant differences based on site of predominant involvement when evaluating mean age (bone: 33.2 vs. soft tissue: 42.9 months; $P = 0.63$), gender (bone, female: 8; bone, male: 9; soft tissue, female, 2; soft tissue, male: 5; $P = 0.41$) or duration of symptoms (bone: 3.5 vs. soft tissue 0.8 months; $P = 0.18$). Patients experienced symptoms for a relatively short duration (mean, 2.7 months; range, 0 to 16 months). This may be due to the young age at presentation, with parents much more readily able to identify a mass in this region than perhaps at other anatomic sites. While there was no statistically significant difference in duration of symptoms based on gender, there was a trend towards females having longer duration of symptoms (females: mean, 4.5; males: mean 1.5 months; $P = 0.07$). There was a statistically significant difference in symptom duration based on side (left: mean, 1.3; right: mean, 5.3 months; $P = 0.02$). None of the patients had any known syndrome association. One patient had a previous head injury [4], while another was diagnosed with asthma [7]. No additional significant clinical findings were identified. Only one patient had multicentric disease [6]. Although patients with multicentric or multifocal infantile

**Table 2** Review of the English literature [4–18]

| Characteristics | Number ($n = 24$) |
|---|---|
| *Gender* | |
| Females | 10 |
| Males | 14 |
| *Age (in months)* | |
| Range | 0–120 |
| Median | 12.0 |
| Mean | 34.8 |
| Mode | Newborn |
| Female (mean) | 38.9 |
| Male (mean) | 31.9 |
| *Symptoms** | |
| Duration (range, in months) | 0–16 |
| Duration (mean, in months) | 2.7 |
| Female patients (mean, in months) | 4.5 |
| Male patients (mean, in months) | 1.5 |
| Left (mean, in months) | 1.3 |
| Right (mean, in months) | 5.3 |
| *Anatomic side* | |
| Left | 16 |
| Right | 8 |
| *Anatomic site** | |
| Lower orbit (eyelid included) | 16 |
| Upper orbit (eyelid and eyebrow included) | 6 |
| Orbital bone predominantly | 13 |
| Orbital soft tissue predominantly | 7 |
| Extension into adjacent structures | 4 |
| *Size (cm)** | |
| Range | 0.2–10 |
| Mean | 3.0 |
| Female (mean) | 1.8 |
| Male (mean) | 3.9 |
| Age $\leq$ 12 months | 3.4 |
| Age $>$ 12 months | 2.5 |
| Bone predominantly | 3.1 |
| Soft tissue predominantly | 2.6 |
| Left | 2.6 |
| Right | 3.7 |
| *Patient follow-up (mean, months)** | |
| A, NED ($n = 18$) | 34.6 |
| A, D ($n = 3$) | 35.0 |
| D, NED ($n = 1$) | n/r |

*A, NED*: Alive, no evidence of disease; *D, NED* Dead, no evidence of disease; *n/r* not reported; * Not provided for all reported cases

myofibromatosis may also have orbital involvement, if orbital disease is the presenting symptom, it seems less likely that the patient will have multifocal or multicentric disease [1, 3, 12]. There have been a few reports of an autosomal-dominant inheritance pattern in four families

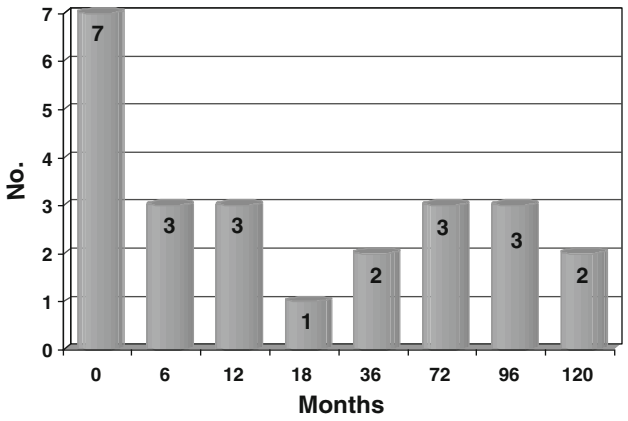


**Fig. 10** Patient age distribution

[1, 22], but these are rare cases seen only in multifocal, systemic infantile myofibromatosis and not in patients with isolated orbital disease. Lastly, although not specifically postulated for orbital lesions, one study suggested that disease development is the result of an increased number of estrogen receptors on smooth muscle cells that may respond in utero to maternal hormones [23].

## Pathologic Features

Although there have been various terms used for this disorder, infantile myofibroma is the currently preferred term [1]. In 1985, Wiswell et al. [24] proposed the following classification scheme:

(1) solitary myofibroma (somatic);
(2) congenital, multicentric myofibromatosis without visceral involvement (multiple, diffuse); and
(3) congenital generalized myofibromatosis with cutaneous and visceral involvement (generalized, somaticovisceral).

This spectrum of disease (solitary, multicentric, generalized) is related to differences in patient outcome. Specifically, if only isolated disease is present, there is a chance of excellent clinical outcome with spontaneous involution [1, 6, 8, 11, 13, 14, 17, 18, 25]. In contrast, patients who have visceral involvement may experience significant morbidity and mortality. In the patient reported herein, there was only isolated orbital disease, and at 12-month follow-up, the residual lesion had undergone spontaneous involution, without need for additional management.

### Macroscopic

Tumors range in size from 0.2 cm up to 10 cm, with a mean of 3.0 cm. The size of tumors is on average larger for

males than females (3.9 cm vs. 1.8 cm; $P = 0.0047$), a finding which was statistically significant. The macroscopic appearance is non-specific, but in general, the lesions are described as being firm, rubbery, and well-circumscribed, although there may be a slightly infiltrative edge. The tumors may be soft at the center and sometimes show areas of degeneration or gelatinous material. They are also often described as "gritty" due to the presence of bone fragments at the edges. Moreover, bone destruction or remodeling is identified in a number of cases.

## Microscopic

Histologically, these tumors are well-circumscribed, although not encapsulated, in the majority of cases; rarely, an infiltrative growth pattern may be seen. The cells are usually arranged in a multilobular appearance, with a biphasic pattern. The two distinct cell populations include plump spindled cells juxtaposed and blended with primitive small round blue cells. The spindled cell component is comprised of a myofibroblastic proliferation of cells with distinct cell borders, abundant cytoplasm, and elongated cytoplasmic extensions tapering out into the stroma. The nuclei vary from cigar-shaped to round to oval or tapering with vesicular chromatin, inconspicuous nucleoli, and no significant atypia. These spindled cells are arranged in bundles, fascicles, or whorled micronodules in a background of collagenized stroma, although isolated cases may have a myxoid appearance. There is a rich vascular network comprised of thin-walled, irregularly branching and occasionally anastomosing vascular spaces often with a gradient characterized by an abundance of vascular spaces concentrated towards the center of the tumor, yielding an appearance similar to hemangiopericytoma [22]. In fact, it is believed that infantile hemangiopericytoma and infantile myofibroma represent different stages of maturation of the same, single entity [26].

The patulous or dilated, staghorn-type spaces are surrounded by a tightly packed primitive or immature-appearing neoplastic population. These cells have a very high nuclear-to-cytoplasmic ratio, lack well-defined cell borders (syncytial architecture), and show scant eosinophilic to amphophilic cytoplasm. Tumor cell spindling can be seen. The nuclei are round to oval, with delicate but still compact nuclear chromatin distribution and generally small and inconspicuous nucleoli. Nuclear pleomorphism is limited to absent, although some cases have been described as having marked pleomorphism focally [26]. These cells are not within the vascular spaces, a feature which can be highlighted with a reticulin stain. Mitoses are identified in most cases, ranging from 1 to 10 mitoses/10 HPFs, and more readily found within these primitive areas rather than within the spindled tumor cells [1].

Vascular space invasion can be seen in a number of cases, as can necrosis [1, 22, 26], although the presence of this feature does not alter the prognosis or outcome. However, the present case did not show either of these features. Hemorrhage can also be seen, along with isolated true calcifications, distinct from the bone fragments commonly present in these tumors. Rarely, osteoclast-like, multinucleated giant cells can be seen [25, 27].

## Histochemical Results

Glycogen may be identified within the spindled lesional cells (usually detected by PAS with and without diastase digestion), but only isolated cells will show a reaction [1, 26], a finding different from other myogenic tumors in the differential diagnosis. Furthermore, a trichrome (Masson or Gomori) stain may be used to highlight fibrous connective tissue (collagen) deposition [1, 12, 22]. Nissl substance or neurofibrils are not identified with Bodian stains or crystal violet stains [1].

## Immunohistochemistry

Vimentin can be seen in all of the lesional cells, whether in the spindled or in the primitive appearing cells. Smooth muscle actin is usually strongly and diffusely present within the spindled population, while staining only focally or less intensely in the primitive cells. In general, a broad panel of other markers tested fails to show any reactivity in either of the populations. These studies include other muscle markers (muscle specific actin, desmin, MYOD1, myogenin), neural markers (S100 protein, GFAP), melanoma markers (HMB-45, melan-A, tyrosinase), and/or epithelial markers (pan-keratin) [2, 6, 7, 10, 11, 13–15, 17, 18, 28]. Isolated cases have shown dot-like cytoplasmic reactivity for low molecular weight keratin in scattered cells [26].

## Electron Microscopy

Electron microscopy has been reported in only a few cases [1, 3, 12, 22, 29]. The cells are described as spindled and round with long cellular processes and extracellular collagen fibrils. The cytoplasm contains fine filaments along with rough endoplasmic reticulum and pinocytotic vesicles. Glycogen and lipid are noted, even though they are not consistently detected by histochemistry studies. Myofibroblastic differentiation is suggested by the sublemmal dense plaque and basal lamina. Apoptotic bodies are frequent, with nuclear fragmentation and engulfment by histiocytes.

## Differential Diagnosis

The differential diagnosis of these lesions includes a variety of reactive lesions and benign and malignant neoplasms. In general, clinical, gross, microscopic, and immunophenotypic findings for each of these lesions is sufficiently distinctive to allow for separation.

Juvenile hyaline fibromatosis is a lesion with similar microscopic findings. However, juvenile (hyaline or desmoid-type) fibromatosis typically occurs after 2 years of age and usually presents within muscle as a solitary lesion. It tends to be less well-circumscribed, shows greater cellularity, tends to involve muscle and periosteum, and is more locally aggressive. Moreover, with juvenile fibromatosis there is no central necrosis, no biphasic appearance, and no hemangiopericytoma-like vascular proliferation. This neoplasm does not resemble smooth muscle.

If only the immature, "small round blue cell" elements are sampled, the differential diagnosis would also include lymphoma (CD45 positive), Ewing/PNET (positive for CD99, FLI1 and *EWS* [22q12] alterations), and neuroblastoma: olfactory neuroblastoma or metastatic neuroblastoma. Both of these latter tumors, however, have very specific neuroendocrine features, including a neural-type matrix, pseudorosettes (Homer Wright rosettes), or true rosettes (Flexner-Wintersteiner), less commonly, and do not show a spindled cell population. In addition, immunoreactivity of the lesional cells for chromogranin, synaptophysin, CD56, and NSE, and S100 protein in a sustentacular pattern would also help with the separation.

Since infantile myofibroma can have intravascular growth, necrosis, and increased mitoses, the differential diagnosis with infantile fibrosarcoma may be a challenge. Infantile fibrosarcoma usually shows a herringbone growth pattern, an inflammatory infiltrate, and may have nuclear atypia. It also shows a distinctive reciprocal translocation, t(12;15)(p13;q25), resulting in *ETV6-NTRK* gene fusion [30]. In some cases, especially with limited sampling, metastatic deposits may be the only way to separate the lesions.

Leiomyoma is a benign smooth muscle tumor which may have a fascicular architecture, but the neoplastic cells are cytologically bland, generally lack necrosis and mitoses, and do not show a hemangiopericytoma-like vascular pattern, nor a biphasic appearance with a primitive cellular component. Similarly, neurofibroma contains bland spindled cells with wavy nuclei arranged in short fascicles, and usually lacks pleomorphism, mitoses, and necrosis. These cells are positive for S100 protein.

Fibrous hamartoma of infancy usually presents in infancy or within the first few years of life. It is a benign, poorly-circumscribed, tumor-like growth comprised of three cellular components: nodules of dense, well-defined bundles of uniform fibrous connective tissue that project into the surrounding fat; primitive fibromyxoid cells arranged in concentric whorls, bands or nests; and intermixed islands of mature adipose tissue. Specifically, it is the intimate relationship with fat that is unique, along with the whorled architecture [31].

Orbital lesions may frequently be associated with bone, and for this reason fibrous dysplasia (showing the characteristic bone formation) and non-ossifying fibroma (storiform growth of fibroblastic-type cells with histiocytes and giant cells) may be considered within the clinical differential diagnosis, but are usually not a major consideration histologically.

Calcifying aponeurotic fibroma tends to develop in older children and shows a strong predilection for the distal extremities. It is intimately associated with dense fibrous connective tissue, displays a fascicular growth of spindled fibroblasts, and occasional epithelioid cells, while showing chondroid foci, with or without calcification [32].

Lastly, but perhaps most importantly, Langerhans cell histiocytosis may yield a solitary lesion around the orbit. In fact, our patient's clinical and radiographic findings at presentation were most suggestive of Langerhans cell histiocytosis. The characteristic collection of histiocytes with associated eosinophils, lymphocytes, plasma cells and isolated multinucleated cells is usually diagnostic. The nuclei are lobular, indented, or folded, showing a coffee-bean shape, with delicate, finely basophilic nuclear chromatin. The cytoplasm is microvacuolated to eosinophilic. The cells are strongly and diffusely immunoreactive with langerin (CD207), CD1a, and S-100 protein.

When taking the orbital location into consideration, some of the histologic differential diagnostic considerations such as nodular fasciitis, digital fibromatosis, fibromatosis coli, and gingival fibromatosis are eliminated from further consideration.

## Treatment and Prognosis

Overall, these lesions are associated with an excellent long-term clinical prognosis. The majority of lesions undergo spontaneous involution or regression with time, despite the initial increase in size. Regression is thought to occur as a result of significant apoptosis [29]. Solitary lesions can recur after excision, which may require quite extensive resection (craniofacial approach, whether open or endoscopic). Local excision with free histologic margins may be difficult to achieve without destructive surgery. Therefore, reconstructive efforts should be planned at the same time (including lacrimal drainage reconstruction). Even though patients with an initial presentation of orbital disease

usually have isolated disease, it is important to evaluate for systemic or multifocal disease with thorough examination and imaging studies, including ultrasound, CT, and MRI. Multifocal or multicentric disease may or may not have visceral involvement. Therefore, it is important to try to determine if additional lesions are present. Finally, there is the multivisceral type in which there is significant visceral involvement by the same process. These lesions are associated with a dismal prognosis (75% mortality rate). With supportive care, however, regression may develop. Several, primarily experimental, treatment modalities, including radiation, localized glucocorticoid injections, and low-dose chemotherapy, have shown benefit in cases of multicentric visceral disease, although experience with these is limited.

## Conclusion

Solitary infantile myofibroma of the periorbital region is an uncommon disorder which presents almost exclusively in children, and is usually an isolated disease. The lesion is more common in male patients, tends to develop on the left side, and is larger in male patients than female patients. The lower orbit is more commonly affected by the biphasic neoplasm. Spontaneous involution is common, but it is important to exclude multifocal or multicentric disease, since the prognosis for multicentric disease is much worse than for isolated cases.

**Acknowledgments** The opinions or assertions contained herein are the private views of the authors and are not to be construed as official or as reflecting the views of the Southern California Permanente Medical Group. The authors wish to thank Dr. Sara Acree for her invaluable copy editing assistance.

**Conflict of interest** There is no financial Conflict of interest.

## References

1. Chung EB, Enzinger FM. Infantile myofibromatosis. Cancer. 1981;48:1807–18.
2. Gopal M, Chahal G, Al-Rifai Z, Eradi B, Ninan G, Nour S. Infantile myofibromatosis. Pediatr Surg Int. 2008;24:287–91.
3. Stout P. Juvenile fibromatoses. Cancer. 1954;7:953–78.
4. Hidayat AA, Font RL. Juvenile fibromatosis of the periorbital region and eyelid. A clinicopathologic study of 6 cases. Arch Ophthalmol. 1980;98:280–5.
5. Stanford D, Rogers M. Dermatological presentations of infantile myofibromatosis: a review of 27 cases. Australas J Dermatol. 2000;41:156–61.
6. Soylemezoglu F, Tezel GG, Koybasoglu F, Er U, Akalan N. Cranial infantile myofibromatosis: report of 3 cases. Childs Nerv Syst. 2001;17:524–7.
7. Westfall AC, Mansoor A, Sullivan SA, Wilson DJ, Dailey RA. Orbital and periorbital myofibromas in childhood: two case reports. Ophthalmology. 2003;110:2000–5.
8. Campbell RJ, Garrity JA. Juvenile fibromatosis of the orbit: a case report with review of the literature. Br J Ophthalmol. 1991; 75:313–6.
9. Duffy MT, Harris M, Hornblass A. Infantile myofibromatosis of orbital bone. A case report with computed tomography, magnetic resonance imaging, and histologic findings. Ophthalmology. 1997;104:1471–4.
10. Galassi E, Pasquini E, Frank G, Marucci G. Combined endoscopy-assisted cranionasal approach for resection of infantile myofibromatosis of the ethmoid and anterior skull base. Case report. J Neurosurg Pediatr. 2008;2:58–62.
11. Larsen AC, Prause JU, Petersen BL, Heegaard S. Solitary infantile myofibroma of the orbit. Acta Ophthalmol. 2010;89(2). doi:10.1111/j.1755-3768.2010.02003.x.
12. Linder JS, Harris GJ, Segura AD. Periorbital infantile myofibromatosis. Arch Ophthalmol. 1996;114:219–22.
13. Nam DH, Moon HS, Chung DH, Baek SH. Solitary infantile myofibroma of the orbital bone. Clin Exp Ophthalmol. 2005;33: 549–52.
14. Persaud TO, Nik NA, Keating RF, Boyajian MJ, Przygodzki RM, Nemi A, et al. Solitary orbital infantile myofibroma: a case report and review of the literature. J AAPOS. 2006;10:283–4.
15. Shields CL, Husson M, Shields JA, Mercado G, Eagle RC Jr. Solitary intraosseous infantile myofibroma of the orbital roof. Arch Ophthalmol. 1998;116:1528–30.
16. Stautz CC. CT of infantile myofibromatosis of the orbit with intracranial involvement: a case report. AJNR Am J Neuroradiol. 1991;12:184–5.
17. Tokano H, Ishikawa N, Kitamura K, Noguchi Y. Solitary infantile myofibromatosis in the lateral orbit floor showing spontaneous regression. J Laryngol Otol. 2001;115:419–21.
18. Waeltermann JM, Huntrakoon M, Beatty EC Jr, Cibis GW. Congenital fibromatosis (myofibromatosis) of the orbit: a rare cause of proptosis at birth. Ann Ophthalmol. 1988;20(10):394–6, 399.
19. Kaplan SS, Ojemann JG, Grange DK, Fuller C, Park TS. Intracranial infantile myofibromatosis with intraparenchymal involvement. Pediatr Neurosurg. 2002;36:214–7.
20. Parker RK, Mallory SB, Baker GF. Infantile myofibromatosis. Pediatr Dermatol. 1991;8:129–32.
21. Williams JO, Schrum D. Congenital fibrosarcoma: report of a case in a newborn infant. AMA Arch Pathol. 1951;51:548–52.
22. Jennings TA, Duray PH, Collins FS, Sabetta J, Enzinger FM. Infantile myofibromatosis. Evidence for an autosomal-dominant disorder. Am J Surg Pathol. 1984;8:529–38.
23. Ikediobi NI, Iyengar V, Hwang L, Collins WE, Metry DW. Infantile myofibromatosis: support for autosomal dominant inheritance. J Am Acad Dermatol. 2003;49:S148–50.
24. Wiswell TE, Sakas EL, Stephenson SR, Lesica JJ, Reddoch SR. Infantile myofibromatosis. Pediatrics. 1985;76:981–4.
25. Gibson SE, Prayson RA. Primary skull lesions in the pediatric population: a 25-year experience. Arch Pathol Lab Med. 2007; 131:761–6.
26. Mentzel T, Calonje E, Nascimento AG, Fletcher CD. Infantile hemangiopericytoma versus infantile myofibromatosis. Study of a series suggesting a continuous spectrum of infantile myofibroblastic lesions. Am J Surg Pathol. 1994;18:922–30.
27. Cruz AA, Maia EM, Burmamm TG, Perez LC, Santos AN, Valera ET, et al. Involvement of the bony orbit in infantile myofibromatosis. Ophthal Plast Reconstr Surg. 2004;20: 252–4.

28. Beham A, Badve S, Suster S, Fletcher CD. Solitary myofibroma in adults: clinicopathological analysis of a series. Histopathology. 1993;22:335–41.
29. Fukasawa Y, Ishikura H, Takada A, Yokoyama S, Imamura M, Yoshiki T, et al. Massive apoptosis in infantile myofibromatosis. A putative mechanism of tumor regression. Am J Pathol. 1994; 144:480–5.
30. Miettinen M. From morphological to molecular diagnosis of soft tissue tumors. Adv Exp Med Biol. 2006;587:99–113.
31. Dickey GE, Sotelo-Avila C. Fibrous hamartoma of infancy: current review. Pediatr Dev Pathol. 1999;2:236–43.
32. Fetsch JF, Miettinen M. Calcifying aponeurotic fibroma: a clinicopathologic study of 22 cases arising in uncommon sites. Hum Pathol. 1998;29:1504–10.